Chapter 6 Chemically functionalized $Ti_3C_2T_x$ MXene for tribo-performance enhancement of castor oil

In this work, we prepared $Ti_3C_2T_x$ MXene from the Ti_3AlC_2 MAX phase by selective etching of Al using a mixture of lithium fluoride and hydrochloric acid etchant. As prepared $Ti_3C_2T_x$ MXene is functionalized with trichloro(octadecyl)silane, which improves the dispersion stability of functionalized MXene (fMXene) in vegetable base oil. The MXene and fMXene are characterized using FTIR, XRD, Raman, XPS, and TEM. There after ASTM D4172B test method was used to analyse the tribological effects of these nanoparticles with increase of concentration on tribological properties of castor oil. The worn surface analysis was conducted by SEM, optical, and stylus profilometry. Their analysis is presented in graphical representation and roughness parameters are used to distinctly identify the mechanism underlying the lubrication enhancement by the fMXene.

6.1. Characterization of materials

6.1.1. **XRD studies**

The XRD pattern of the Ti_3AlC_2 MAX phase (Figure 6.1) exhibits diffraction peaks at 2θ values of 9.4°, 19.1°, 33.8°, 38.9°, 41.7°, 48.6°, and 56.4°, corresponding to the crystalline planes (002), (004), (103), (104), (105), (107), and (109), respectively. In this phase, layers of aluminum atoms are positioned between the Ti_3C_2 lamellae with a major peak present at 38.9°, binding titanium carbon together through metallic bonds. The Al is removed from the MAX phase by the etching which creates a gap between the lamellar structures. This results to increase in spacing between lamellae, consequently, there is a decrease in the diffraction angle of (002) plane which appeared at 5.84°. After functionalization, the (002) peak is minutely shifted to 2θ of 6.37°.

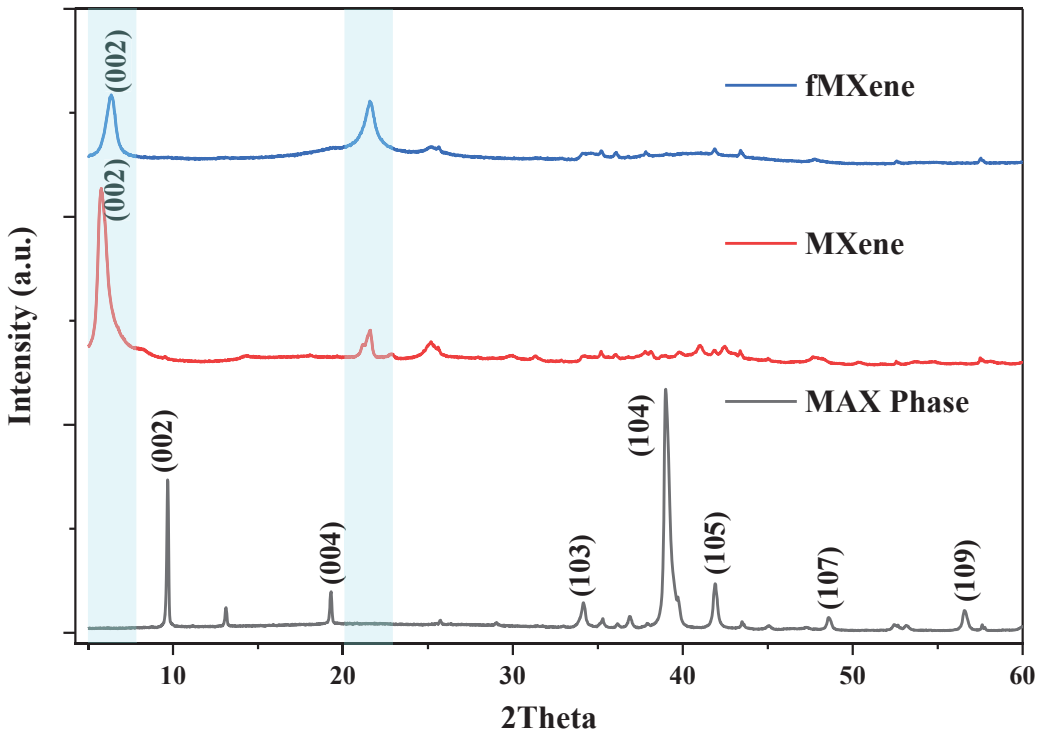

Figure 6.1: XRD scans from 5 to 60 of MAX Phase, MXene and fMXene

6.1.2. **FTIR studies**

The chemical functionalities of the Ti_3AlC_2 MAX phase, $Ti_3C_2T_x$ MXene, and functionalized $Ti_3C_2T_x$ MXene (f-MXene) nanocomposites were analyzed using FTIR spectroscopy. The FTIR spectrum of the Ti_3AlC_2 MAX phase (Figure 6.2) reveals no significant vibrational peaks, except for a weak bending mode at around 1630 cm^{-1}, which is attributed to the bending of adsorbed water (δH_2O) on the surface of Ti_3AlC_2. The FTIR spectrum of $Ti_3C_2T_x$ MXene displays several characteristic peaks. A broad and intense band at 3439 cm^{-1} is attributed to the O-H stretching vibrations of hydroxy groups on the surface, while a peak at 1631 cm^{-1} corresponds to the bending mode of adsorbed water molecules (δH_2O) [111]. Additionally, a band at 557 cm^{-1} is observed, which is associated with the Ti-O stretch, representing oxygen functionalities on the Ti layers of $Ti_3C_2T_X$. Upon functionalization with trichloro(octadecyl)silane (OTS), the FTIR

spectrum of the modified $Ti_3C_2T_x$ MXene shows new peaks. The peaks at 2924 and 2852 cm^{-1} correspond to the asymmetric and symmetric stretching vibrations of the CH_2 groups in the alkyl chain of OTS, confirming the presence of the long alkyl chain. A peak at 1125 cm^{-1} is also observed, which is assigned to the Si–O–Ti bond, indicating the successful grafting of OTS onto the MXene surface through the formation of a stable Si-O-Ti linkage. These FTIR results confirm the chemical modification of $Ti_3C_2T_x$ MXene with OTS, demonstrating the attachment of silane molecules and the formation of Si-O-Ti bonds on the MXene surface [112].

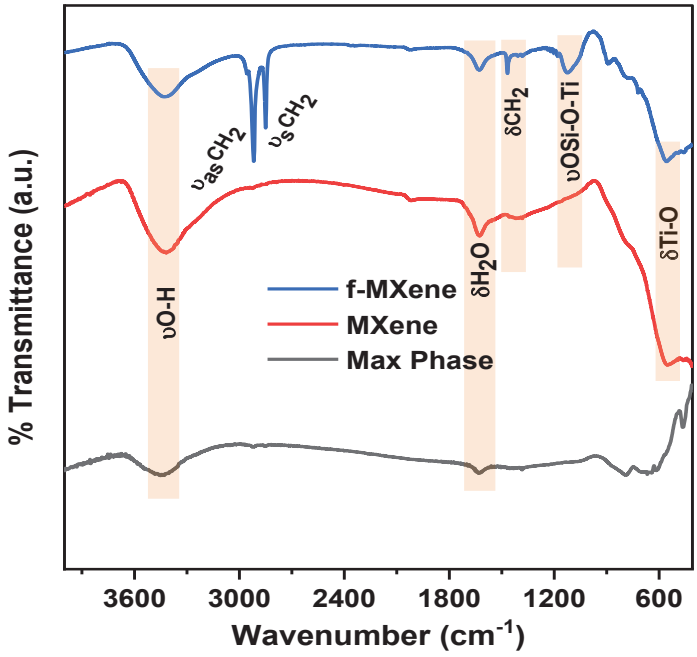

Figure 6.2: FTIR of powder samples in a spectracl range of 4000 to 400 cm^{-1}

6.1.3. **Raman studies**

The Raman spectrum of the Ti_3AlC_2 MAX phase (Figure 6.3a) exhibits distinct vibrational modes of Ti-Al and Ti-C linkages. Spectral peaks in the lower wavenumber region (270-700 cm^{-1}) correspond to these vibrations, confirmed the presence of the MAX phase [113,114]. Notably, the absence of D- and G-bands (typically associated with graphitic structures) suggests an ordered crystalline structure without significant

carbonaceous impurities. Upon selective etching of aluminum (Al) from the MAX phase, the Raman spectrum of $Ti_3C_2T_x$ MXene (Figure 6.3b) shows significant structural modifications [115]. The disappearance of Ti-Al peaks, along with the emergence of D (1315 cm^{-1}) and G (1554 cm^{-1}) bands, indicates the formation of graphitic carbon domains and surface terminations. Additionally, the Ti-C vibrations persist but exhibit slight shifts due to interactions with terminating groups (-OH, -F, -O). The broadening of spectral features suggests increased disorder, likely attributed to the delamination process [116].

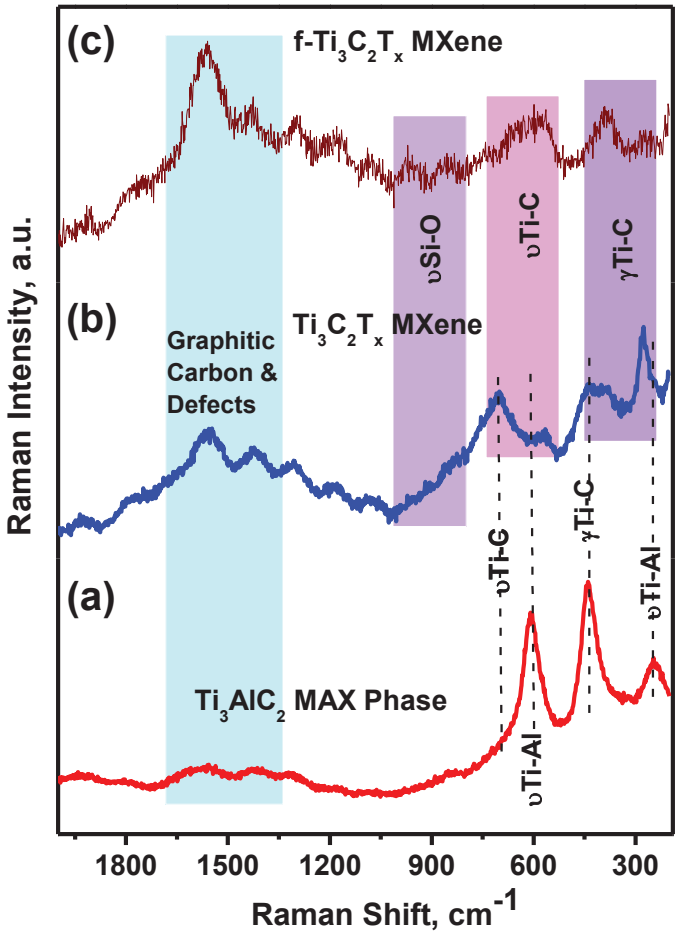

Figure 6.3 Raman spectra of chemically functionalized f-$Ti_3C_2T_x$ MXene at different synthesis stages, including the pristine Ti_3AlC_2 MAX phase and $Ti_3C_2T_x$ MXene

The functionalization of MXene is confirmed by further evolution in the Raman spectrum of f-MXene (Figure 6.3c). The appearance of Si-O vibrational modes (800-1000 cm^{-1}) validates the successful grafting of octadecyltrichlorosilane (OTS) onto the MXene surface. Importantly, the retention of Ti-C peaks demonstrates that the core MXene structure remains intact despite surface modification. Furthermore, the presence of D and G bands suggests minor structural perturbations but no substantial degradation of the material. The disappearance of Ti-Al peaks, the emergence of graphitic carbon-related bands, and the presence of Si-O modes provide clear evidence of synthesis and chemical modification in the f-$Ti_3C_2T_x$ MXene [117].

6.1.4. **Morphology of particles**

Figure 6.4 shows the Transmission electron microscopic (TEM) images of MAX phase, MXene and fMXene. The images of MAX phase show the bulk nature of the particles. These bulky particles are stacked by laminated layers of the M (Ti), A (Al) and X (C). Fifty to sixty layers are visible in Figure 6.4b in laminated form. After the removal of Al, the intercalated hydroxyl group in MXene reduces the number of layers into few laminates, which is also depicted from Figure 6.4e. Figure 6.4g, h depicted highly dispersed particles across the area with lamellar sheets. Distinct ring pattern of polycrystalline nature is depicted in selected area electron diffraction (SAED) pattern shown in Figure 6.4c. The bright spots superimposed on the rings might indicate the presence of crystalline domains within the material. Figure 6.4f shows the diffuse ring pattern suggest less ordered structure whereas Figure 6.4i shows distinct ring pattern which indicates increase in order of the structure.

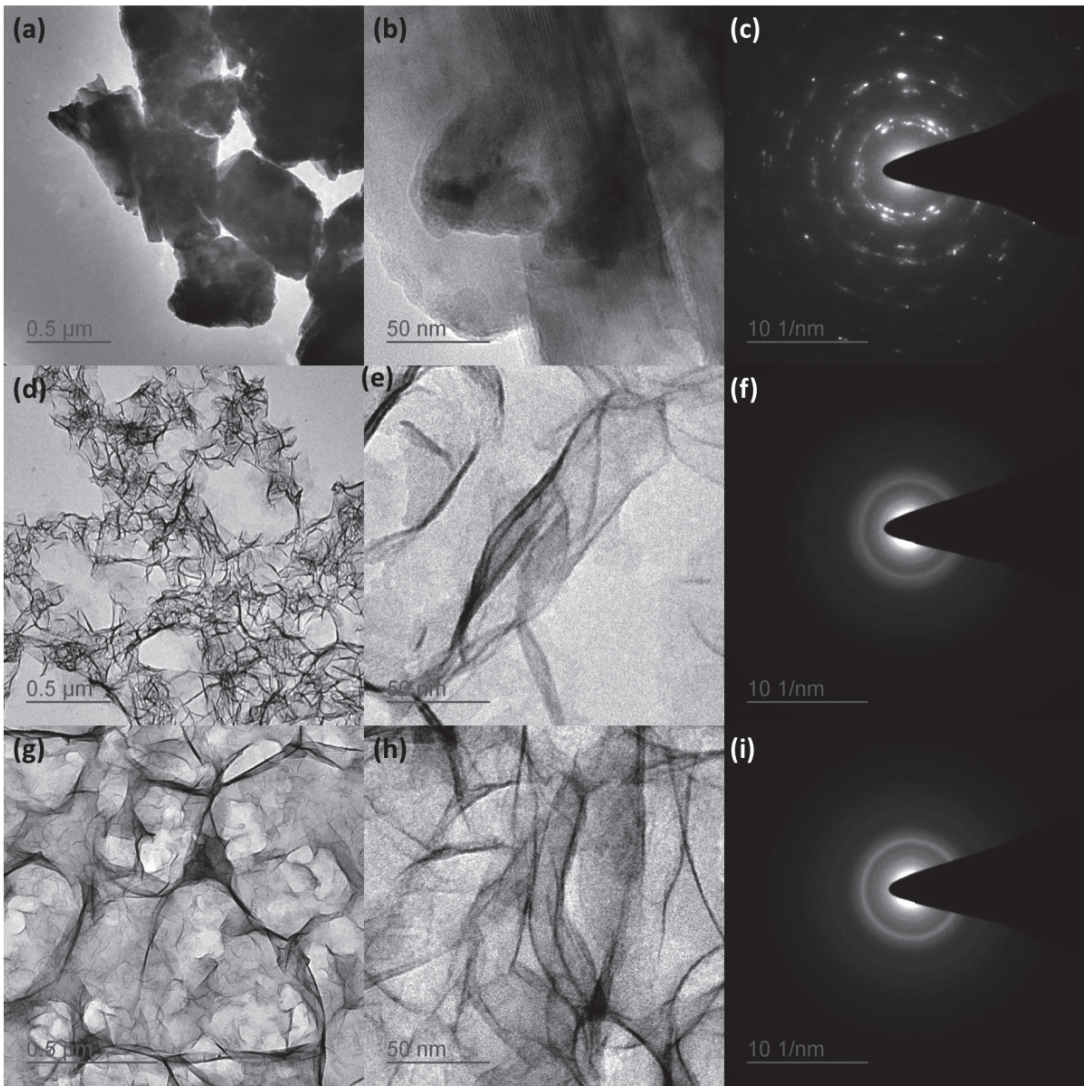

Figure 6.4 Transmission electron microscopic images and selective area electron diffraction of (a, b, c) MAX Phase; (d, e, f) MXene; (g, h, i) functionalized MXene (fMXene)

6.2. Dispersion stability

Figure 6.5 shows the digital images of nanolubricant dispersed in the castor oil over time. The dispersion stability of MXene and functionalized MXene (fMXene) with time can be assessed. The 0.025, 0.05, 0.075 and 0.1 wt% concentration of nano lubricant is dispersed in to castor oil. The 0.1 wt% concentration of the lubricant samples are kept undisturbed to check for dispersion stability. The higher concentration is chosen as the agglomeration

will be clearly visible at higher concentration. From the images it is clearly visible that the agglomeration of MXene at the bottom of the vial is after 3 days. The fMXene added lubricant shows no sign of agglomeration after 3 days. Moreover, samples were again kept for another 6 days, then 12 days. After 12 days the MXene deposits a thick layer at the bottom, where asthe fMXene forms a small thin layer at the bottom. This result suggests greater dispersion stability of functionalized MXene.

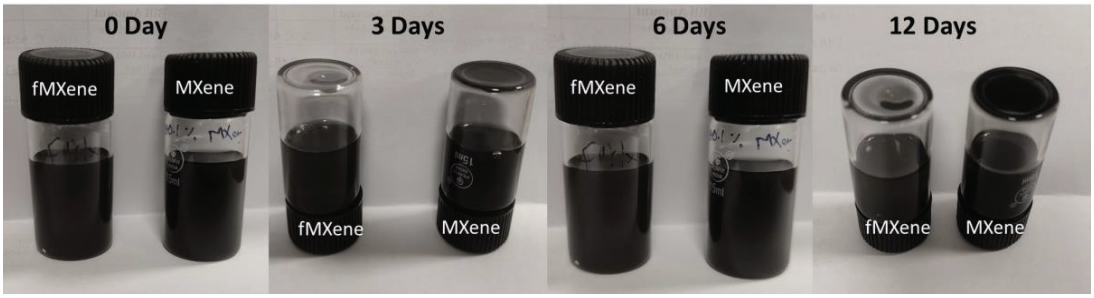

Figure 6.5 Digital images of lubricants showing dispersion stability in castor oil with time

6.3. Tribological tests of lubricant

Tribological test results depicted in Figure 6.6 shows the reduction in coefficient of friction with addition of nanoparticles. The interaction of asperity is prominent in boundary regime with thin film of lubrication which bears high load around 3.4 G Pa Hertzian contact pressure in case of ASTM D 4172B. Interaction of nano particles becomes important in this regime. The MXene having layered 2D structure with strong tensile strength and low inter-laminar shear strength [118] eases the movement between tribo-surfaces, resulting in reduction of coefficient of friction. There is an increase in coefficient of friction with increase in concentration of additives. 0.025 wt% of fMXene in castor oil shows optimal behaviour. In comparison to pristine MXene, the functionalized MXene show better performance at all concentrations. Figure 6.7 shows the changes in coefficient of friction vs time for all lubricants. Smooth curves are

assigned to fMXene blended lubricants whereas for MXene blended lubricants there is deviations in friction curve with concentration. The agglomeration of nano-lubricants between surfaces can cause deviations in performance. Homogeneously dispersed lubricants, on the other hand, facilitate a smooth friction curve over time. Intermittent breakdowns in the lubrication film increase friction between tribo-pairs, resulting in enhanced wear.

Figures 6.8a and 6.8b illustrate the variation in wear scar diameter and corresponding wear volume, respectively. The addition of nano-lubricants yields a reduction in wear. However, as the concentration of additives increases, wear volume also increases. The surge in wear volume can be attributed to the harsh abrasion caused by the increased particle concentration, which acts as a third body between the tibo-surfaces. The fMXene having the functionality of eighteen carbon chain with polar ends helps the particles to be dispersed and acted properly on the worn surface. The polar functionality increase interaction with metallic surface whereas the M and X layers of MXene helps in tribo film formation. Deposition of nano-lubricant at the interacting surface causes reduction in wear volume. Further investigation is required for justification of film deposition and tribolayer formation.

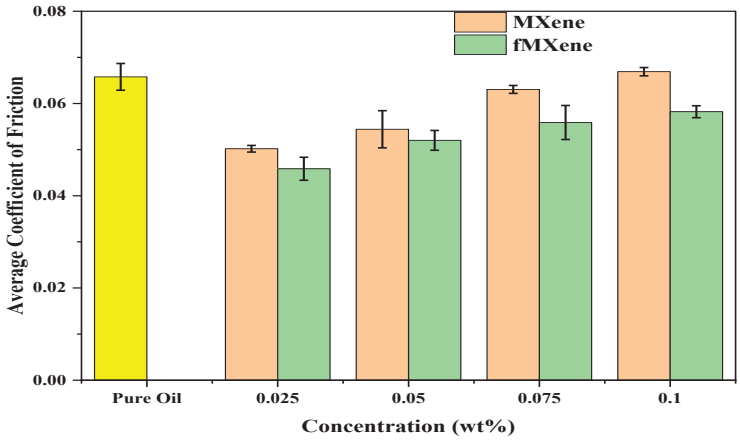

Figure 6.6: Average coefficient of friction of different lubricant at specified percentage weight (wt%)

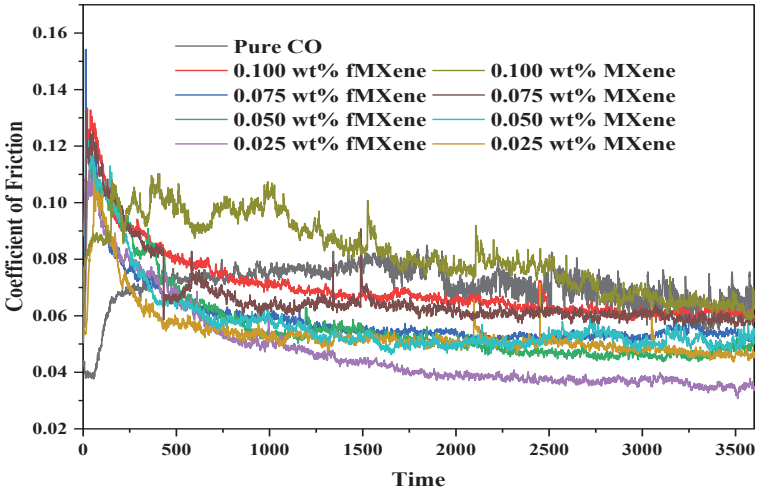

Figure 6.7: COF vs time plot of different nano lubricants

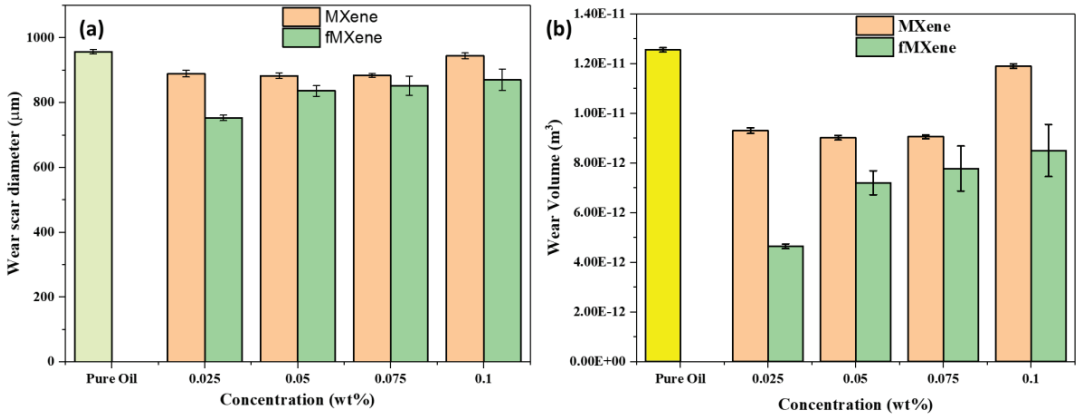

Figure 6.8: Change in (a) wear scar diameter and (b) wear volume with concentration of additives

6.4. Worn surface analysis

6.4.1. SEM and EDS

Figure 6.9 shows SEM images of worn scar developed on steel balls under different lubrication system. There is a reduction in wear scar diameter as we move from Figure 6.9a to (c) which shows the effective antiwear performance of fMXene. The point and area scan of the worn surface is done using energy dispersive spectroscopy (EDS) shown in Figure 6.10. The worn surface lubricated by nano additives shows deposition of tribofilm on to the surface which is held responsible for reduction in valley height in R_{vk} (Figure 6.11). The functionalized MXenes possess abundant active sites due to their chemically functionalized terminal groups. These terminal groups enhance the interaction of MXene particles with the metal surface, facilitating stronger adsorption. The polar functionalities contribute to this process by forming a thin film on the substrate, thereby intensifying the element's surface presence. The enhanced interaction aids in anchoring the fMXene particles onto the surface, forming a stable tribofilm. Additionally, the lamellar structure of MXenes allows them to align parallel to the metal surface, reducing friction due to easy shearing between their layers.

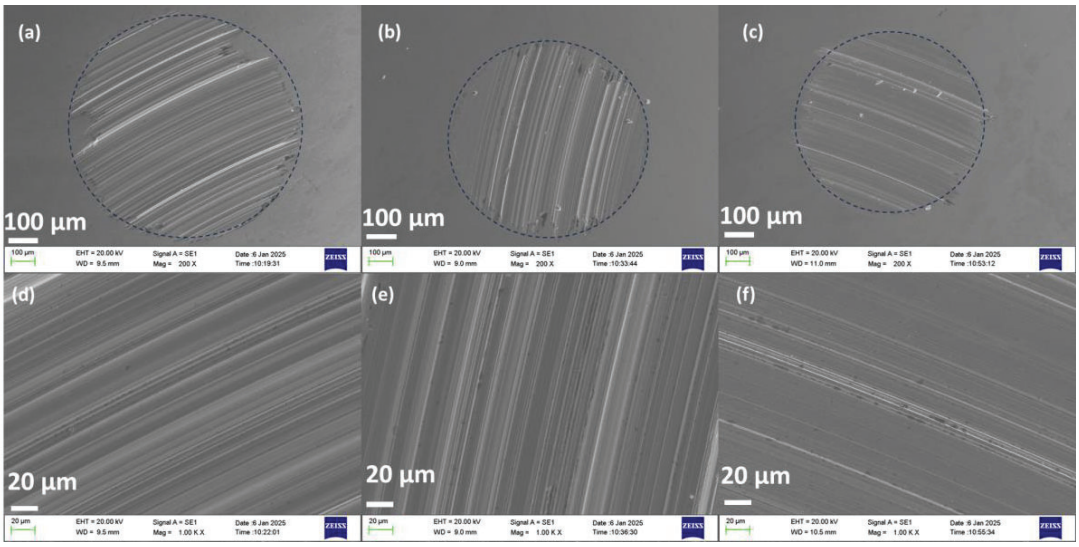

Figure 6.9: SEM images of scar surface for worn steel balls lubricated with (a, d) Pure castor oil, (b, e) 0.025 wt% MXene nano lubricant, (c, f) 0.025 wt% fMXene nano lubricant

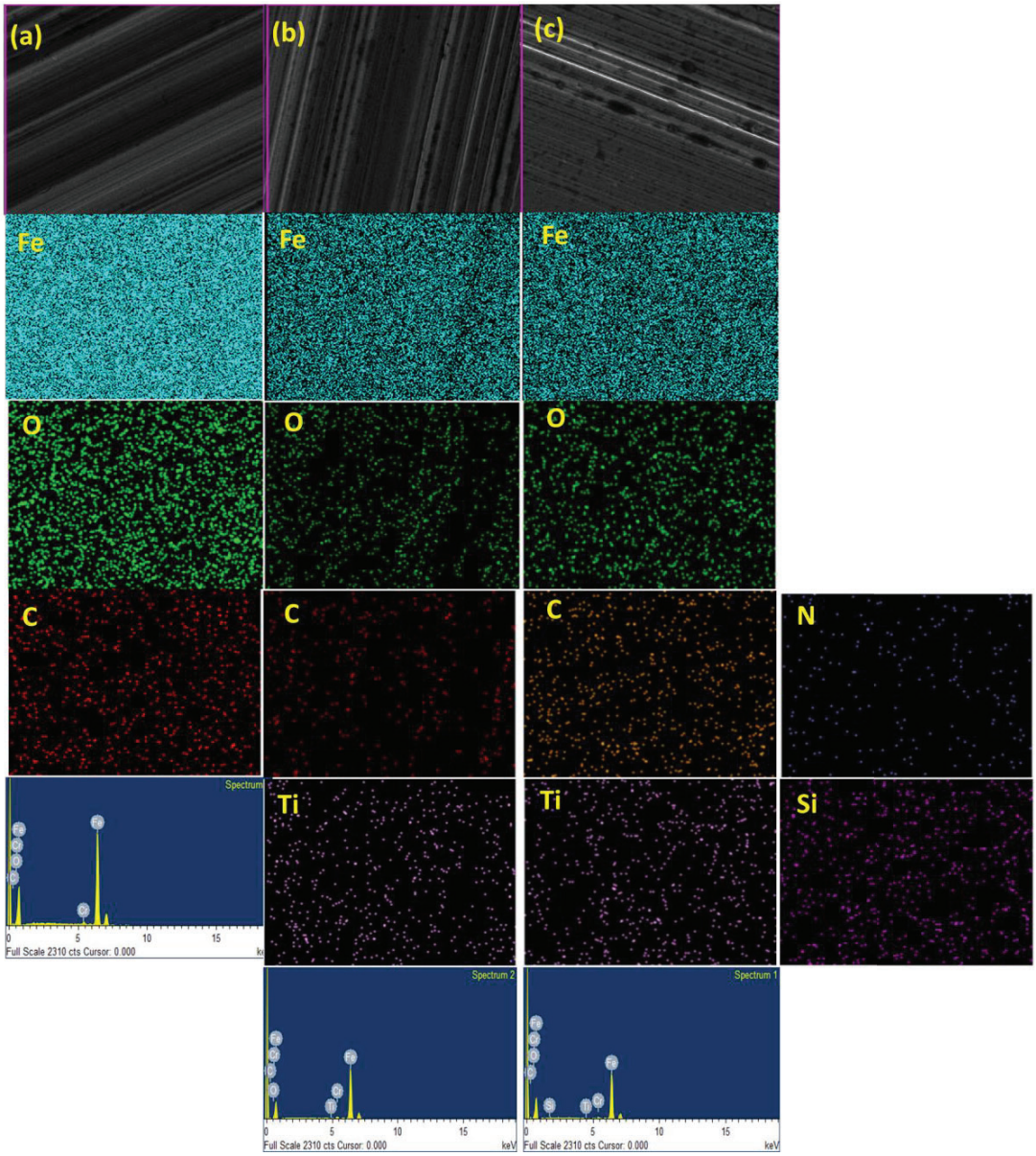

Figure 6.10: EDS mapping and spectrum of different worn surfaces tested with (a) pure CO, (b) 0.025 wt% MXene nanolubricant, (c) 0.025 wt% fMXene nanolubricant

6.5. Roughness data analysis

Figure 6.11(a-c) illustrates the roughness parameter with material ratios also known as bearing ratio curve. The R_{pk} represents the average peak height and R_{vk} is the representation of valley depth. The M_{r1} and M_{r2} represent the material limit for contacting surfaces. The difference of material limit represents the effective bearing length which is

increased when we move from (a) to (c). There is a reduction in valley depth as we move from (a) to (c) which shows the reduction of depth on the worn surface. The reduction in depth can be caused by filling of valley by nanolubricant particles. This effect is mending and it is more prominent for the case of functionalized MXene (fMXene) as additive. Figure 6.10d, e, and f shows the fractal analysis of the worn surface collected from box counting method, the average fractal dimensions (FD) of three different line profiles are shown in Figure 6.11 as FD, which depicts there is reduction in FD with MXene lubricated scar surface but it increases again for the case of scar surface lubricated with fMXene.

$$FD = \frac{log(number\ of\ self\ similar\ pieces)}{log(magnification\ factor)} \qquad 6.1$$

The increase in fractal dimension signifies the increase in self-similar pieces in the surface. The self-similar surfaces signify the homogenous rubbing throughout the surface. The MXene added lubricants due to agglomeration there is an uneven rubbing on the surface which reduces the fractal dimensions of the worn scar surface.

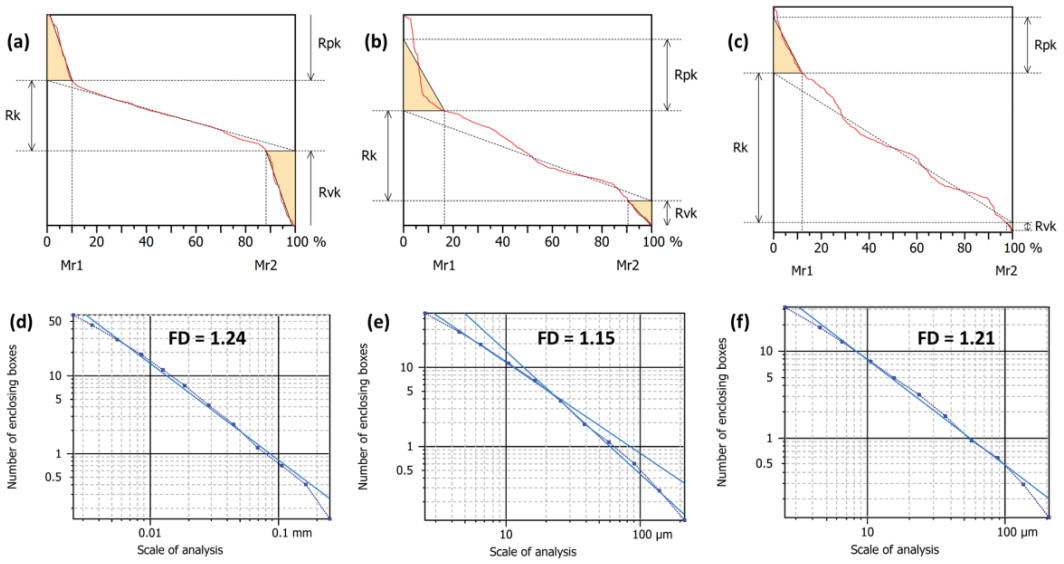

Figure 6.11: Bearing ratio curve by R_k parameter and corresponding Fractal dimension (FD) of scar surface tested by (a, d) Pure castor oil, (b, e) 0.025 wt% MXene blended nano lubricant, (c, f) 0.025 wt% fMXene blended nano lubricant

Figure 6.12 presents the optical 3D profilometry results for the worn surfaces of tested balls under different lubrication conditions. The accompanying table provides the line roughness measured along the wear scar perpendicular to lay line and the surface roughness of the extracted worn area, which encompasses approximately 80–90% of the worn region, excluding the edges. Both surface and line roughness exhibit a similar trend, showing a progressive reduction from the wear scars lubricated with pure oil to those lubricated with MXene and finally to fMXene. This reduction in roughness signifies the polishing effect of the nanolubricants, with the fMXene-lubricated surface demonstrating the most effective polishing performance.

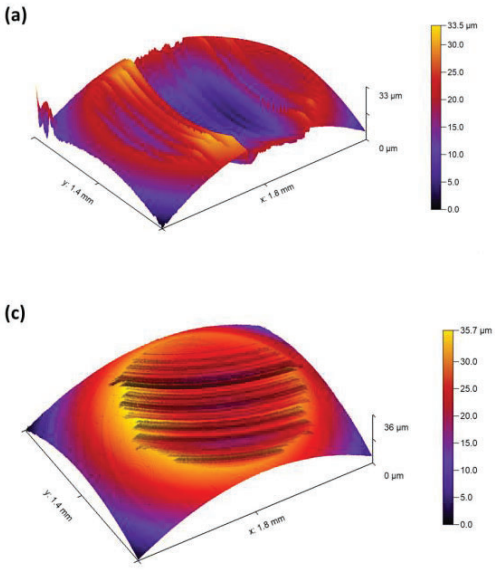

Sample	Line Parameter	Value (µm)	Surface Parameter	Value (µm)
(a)	Ra	1.196	Sa	5.39911
(a)	Rq	1.646	Sq	6.38049
(a)	Slope	0.231		
(b)	Ra	0.862	Sa	2.47844
(b)	Rq	1.145	Sq	3.07789
(b)	Slope	0.1388		
(c)	Ra	0.741	Sa	2.16695
(c)	Rq	0.954	Sq	2.73086
(c)	Slope	0.1306		

Figure 6.12: 3D optical profilometry images along with line and surface roughness parameter values in table for worn scar surfaces lubricated with (a) Pure Castor Oil, (b) 0.025 wt% MXene nano lubricant, (c) 0.025 wt% fMxene nano lubricant

6.6. Chapter summary

This chapter explores the synthesis, functionalization, characterization, and tribological evaluation of MXene nanoparticles as lubricant additives. MXene was prepared from the Ti_3AlC_2 MAX phase using selective etchant, i.e., mixture of lithium fluoride and hydrochloric acid, followed by functionalization with OTS to enhance dispersion stability in castor oil. XRD analysis revealed shifts in the (002) diffraction peak, indicating increased interlayer spacing after. FTIR confirmed successful functionalization through the presence of Si–O–Ti bonds and alkyl chain vibrations. TEM images showed a reduction in lamellar thickness after etching. Dispersion stability tests demonstrated that functionalized MXene (fMXene) exhibited significantly improved stability, remaining well-dispersed for over 12 days compared to pristine MXene, which settled within 3 days. Tribological tests (ASTM D4172b) revealed reduced coefficient of friction (COF) and

wear with both MXene and fMXene, with optimal performance observed at 0.025 wt% fMXene. The enhanced lubrication was attributed to the formation of stable tribofilms and uniform dispersion, resulting in smoother friction curves and superior antiwear properties.

Worn surface analysis using SEM, EDS, and profilometry confirmed reduced wear scar diameters, lower valley depths (Rvk), and effective tribofilm formation with fMXene. Fractal analysis revealed improved surface homogeneity, whereas the 3D profilometry highlighted significant reductions in surface roughness. Overall, the functionalization of MXene improved its tribological performance, making it a promising additive for advanced lubrication applications, with potential for further exploration of tribolayer mechanisms.